

Multiple Posttranslational Modifications at Distinct Sites Contribute to Heterogeneity of the Lipoprotein Cytochrome *bo*₃[†]

Alexander Prutsch,[‡] Christiane Lohaus,[§] Brian Green,^{||} Helmut E. Meyer,[§] and Mathias Lübbers^{*,‡}

Lehrstuhl Biophysik and Institut für Physiologische Chemie, Ruhr-Universität Bochum, Universitätsstrasse 150, D-44780 Bochum, Germany, and Micromass UK Ltd., Floats Road, GB-Manchester M23 9LZ, United Kingdom

Received September 21, 1999; Revised Manuscript Received February 14, 2000

ABSTRACT: The heme-copper cytochrome oxidase of *Escherichia coli* (cytochrome *bo*₃) was tagged with oligohistidine at the C-terminus of the small noncatalytic subunit IV. After detergent solubilization, the enzyme was purified by a one-step procedure with immobilized metal affinity chromatography. Using different cytochrome *bo*₃ constructs as reference, the products were investigated by mass spectroscopical and immunological methods. Several posttranslational modifications of subunits II, III, and IV were observed: (1) N-terminal methionines of subunits III and IV are split off. (2) Fifty percent of subunit III polypeptides are acetylated, presumably at the N-terminal alanine. (3) Lipoprotein processing of subunit II involves cleavage of the signal peptide. (4) Maturation of subunit II [Ma, J., Katsonouri, A., and Gennis, R. B. (1997) *Biochemistry* 36, 11298–11303] alters the structure of the N-terminal cysteine by N-palmitoylation and S-glyceryldipalmitoylation. (5) A hexapeptide is split off from the C-terminus of subunit II. This happens subsequently to the N-terminal lipoprotein processing step and is dependent on the growth state of cells.

Cytochrome oxidases are integral membrane proteins of energy-transducing membranes, which catalyze the terminal reduction of dioxygen via electron transfer from donor substrates. Cytochrome *c* or ubiquinol oxidases belong to the so-called superfamily of heme-copper oxidases, which has members in all known groups of organisms, i.e., eubacteria, eukaryotes, and archaea (1–4). In bacteria, the oxidases are located in the cytoplasmic membrane. The hetero-oligomeric enzymes regularly consist of a catalytic subunit I composed of 12–15 transmembrane helices, which binds the redox cofactors noncovalently, namely, the low- and high-spin hemes of the A-, B-, and O-type, as well as the so-called Cu_B. Heme *a*₃ (or *o*₃) and Cu_B together form the binuclear reaction center, where molecular dioxygen is bound, which is subsequently reduced to water (5). Subunit II has a membrane anchor composed of two transmembrane helices and a C-terminal hydrophilic domain that faces to the periplasmic space (6–8). In cytochrome *c* oxidases, a part of the surface of subunit II seems to form the binding site for the macromolecular substrate, cytochrome *c* (9, 10). Its polar domain provides histidine and cysteine ligands for another copper redox center, termed Cu_A (11). These ligands are absent for the quinol oxidases (12–15), whose substrate binding site(s) is (are) less clearly defined (cf. to ref 16).

The exact function of subunit III is not known; it may play a role in the biosynthesis or the assembly of the complex (17–19). The same may hold for subunit IV found in bacterial ubiquinol oxidases (19–21). A fifth gene found in bacterial oxidase operons (22) encodes a farnesyltransferase, which is important for the biosynthesis of the high-spin heme; the protein could be a loosely or transiently associated structural component of the cytochrome *bo*₃ complex (23).

Microbial cytochrome oxidases have been purified either as such (13, 14, 23–29) or after protein redesigning by virtue of oligohistidine tags added to the C-terminus of different subunits (30–33). In the latter case, the advantage of greater ease in purification via a one-step procedure is evident. For the purpose of studying structure–function relationships of the isolated cytochrome *bo*₃, we reconstructed the C-terminus of subunit IV by addition of an oligohistidine tag. During analysis of the product, we observed a significant band inhomogeneity of the subunit II polypeptide. This has lead us to a thorough protein chemical characterization of the preparation. Using biochemical methods and, in particular, the electrospray ionization (ESI) mass spectroscopical technique, we discovered certain new posttranslational modifications at different sites of the protein.

MATERIALS AND METHODS

Genetic Constructs. Constructs are based on the pBR322-derived plasmids pMC39 (34) and pRCO1 (35), kind gifts of Prof. Robert Gennis, Urbana. The vector pHTAG, coding for a hexahistidine oligopeptide at the 3'-end of *cyoD* (Figure 1) was constructed by PCR mutagenesis using the overlap extension protocol (36). At the first stage, the primer pairs ESHT/3HTAG2 and 5HTAG2/SPHT (Table 1; primer

[†] Supported by the Deutsche Forschungsgemeinschaft, Grant SFB 394-C6 to M.L.

* To whom correspondence should be addressed. Telephone: +49-234-32-24465. Fax: +49-234-32-14626. E-mail: luebben@bph.ruhr-uni-bochum.de.

[‡] Lehrstuhl Biophysik, Ruhr-Universität Bochum.

[§] Institut für Physiologische Chemie, Ruhr-Universität Bochum.

^{||} Micromass UK Ltd.

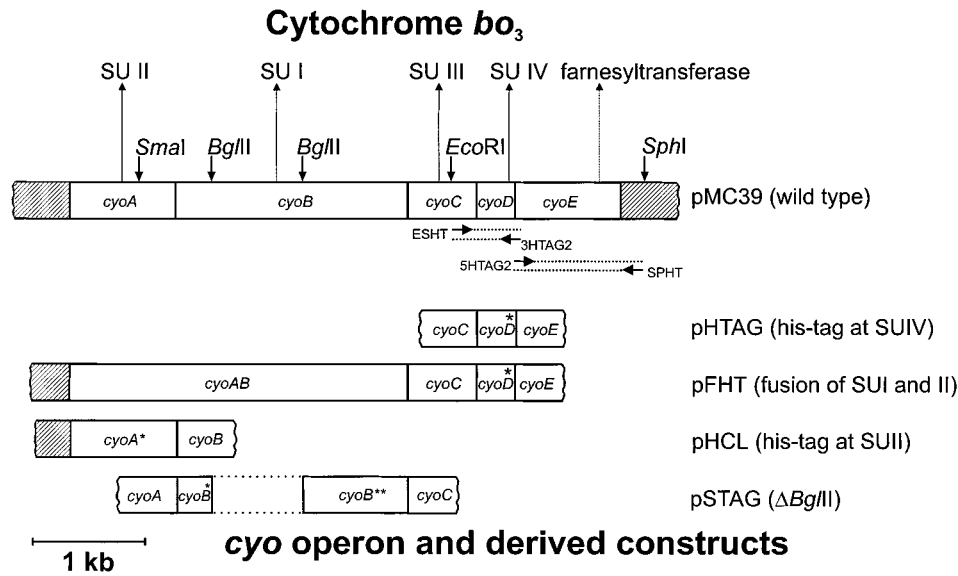


FIGURE 1: Maps of the *cyo* operon and the derived plasmid constructs. Only the *cyo* region of the pBR322-derived constructs [mother plasmid pMC39 (34)] are shown. Short arrows point to singular restriction sites, and long arrows point to the related gene products. Positions of the PCR primers for encoding the oligohistidine tag are indicated.

Table 1: Oligonucleotide Primers Used for Overlap Extension PCR ^a	
5HTAG2	caccaccaccaccactaagagcggcggttatga
3HTAG2	gtggtggtggtggtggtgcatcatcatgttga
SPHT	cgcgcatgcgcaacgagaatacg
ESHT	tatgaattccatcacctgatt

^a The recognition site of *Eco*RI is italicized in primer sequences.

concentrations, 1 μ M) each were mixed in a total volume of 100 μ L with reaction buffer, 50 ng pMC39, 200 μ M of the four 3'-deoxynucleotides, and 2.5 U of *Pwo*-Polymerase (Boehringer Mannheim); thermocycling conditions were one 3-min, 96 $^{\circ}$ C denaturation; 30-s, 46 $^{\circ}$ C annealing; and 1-min, 72 $^{\circ}$ C extension, followed by 25 cycles of 1-min, 94 $^{\circ}$ C denaturation; 30-s annealing; and 1-min extension, followed by a final 10-min extension step. The resulting fragments of 0.6 and 1.1 kb size were gel-purified and extracted with the Qiaex kit (Qiagen) in a volume of 20 μ L of 10 mM Tris-HCl and 1 mM EDTA, pH 8.0 (TE buffer). In the second stage, 1 μ L of these overlapping fragments was combined as templates with primer pair ESHT/SPHT and reactants as described before. The PCR conditions were as above, except that the extension times were 1.5 min for the resulting 1.7-kb fragment. The fragment was ligated into pMC39 cut with *Eco*RI and *Sph*I (Figure 1) and transformed to *E. coli* XL1-blue (Stratagene) to result in pHTAG. The construct was verified by DNA sequencing. The plasmid pSTAG carrying a defective *cyoB* gene was generated by deletion of the internal *Bgl*III fragment (0.8 kb, see Figure 1) from pHTAG followed by religation.

The construct pFHT is based on pHTAG (histidine-tagged at subunit IV) and bears a fusion of genes encoding subunits I and II generated by moving of the *Sma*I/*Eco*RI fragment of pRCO1 into pHTAG (Figure 1). The presence of both *cyoAB* fusion and histidine codons was demonstrated by DNA sequencing. pHCL is a vector encoding a subunit II-tagged cytochrome *bo*₃ variant (kindly obtained by Dr. Anne Puustinen, Helsinki), which was preliminarily characterized earlier (37). In *E. coli* strain BL21 Δ *cyo recA*⁻, the *cyoBCD* genes are replaced by a kanamycin resistance factor cassette, and the *cyd* operon encoding the alternative oxidase is kept

intact. These features allow expression of plasmid-encoded mutant genes that cause nonfunctional oxidases.

Strain JM107 $\Delta\Delta$ carries the same *cyoBCD* chromosomal deletion; in addition, its *cydAB* operon is inactivated by insertion of a chloramphenicol resistance factor gene. Because of the double mutation of oxidase genes, the latter strain is respiration-deficient and serves as an indicator strain for aerobic complementation experiments (details on the construction will be given elsewhere).

Fermentation of *E. coli*—Expression of Oxidase. The ampicillin resistance conferring plasmids pMC39, pHTAG, pSTAG, pFHT were transformed into *E. coli* strain BL21 Δ *cyo recA*⁻. Cells were grown at 37 $^{\circ}$ C in Luria–Bertani medium, pH 7.5, and 0.1 mg/mL ampicillin using conical flasks indented for better aeration at 100 rpm in a gyratory shaker. For large-scale fermenter cultivation, 1 L of a preculture grown as described above was used to inoculate 26 L of medium, supplemented with 1 mL of Antifoam 289 (Sigma), aerated with 24 L of air per minute, and mixed with a stirrer frequency of 600 rounds/min. The pH was adjusted to 7.5 by the addition of HCl or NaOH. After the optical density at 560 nm reached 4.2 (usually after 18 h), the cells were harvested and stored at -20° C until use.

Purification of the Histidine-Tagged Oxidase. For preparation of cytoplasmic membranes, 90 g of wet cell material of *E. coli* were thawed, resuspended in ice-cold TE buffer, and broken by ultrasonic oscillation for 60 min at output level 8, 50% duty cycle (Sonifier 250, Branson) under chilling with ice. Cell debris was removed by twice centrifuging at 15 100 rpm in a SS34 rotor (Sorvall) at 4 $^{\circ}$ C for 10 min. Crude membranes were pelleted from the supernatant by ultracentrifugation for 50 min at 4 $^{\circ}$ C at 40 000 rpm in a 45 Ti rotor (Beckman). To remove loosely bound proteins, the red-brownish material was homogenized in TE buffer, the same volume of 10 M urea was added, and the mixture was centrifuged as above at 15 $^{\circ}$ C. Washed membranes were resuspended in 4 mL of TE buffer. The oxidase was solubilized by the addition of 2 mL of 0.5 M potassium phosphate, pH 8.0, 2 mL of 10% (w/v) Triton-X 100, 5 mL

of 10% (w/v) *N*-octyl- β -D-glucoside (Bachem), 1.5 mL of 4 M NaCl, and 5.5 mL of deionized water to 4 mL of membrane suspension. The mixture was stirred for 30 min at room temperature and centrifuged in a 75 Ti rotor (Beckman) for 40 min at 40 000 rpm at 4 °C.

A Ni²⁺-NTA agarose column (Qiagen) was freshly poured after overnight preequilibration (4 °C) of 6 mL of bead suspension with 40 mL of 50 mM potassium phosphate, pH 8.0, 300 mM NaCl, and 0.3% (w/v) β -D-decylmaltoside (Bachem) (wash buffer) and loaded with the membrane detergent extract at a flow rate of 0.5 mL/min. To remove loosely bound proteins, first, 12 mL of wash buffer, then 24 mL of 10 mM imidazol, and finally 12 mL of 20 mM imidazol in wash buffer were passed over the column. The oxidase was eluted with 6 mL of 100 mM imidazol in wash buffer, and it was concentrated with Microsep centrifugal ultrafiltration tubes (Pall) for 2 h at 5000 rpm in a SS34 rotor at 4 °C. To get rid of the major portion of imidazol from the elution buffer, the sample was diluted by adding a 20-fold volume of 20 mM Tris-HCl, 50 mM NaCl, and 0.3% (w/v) β -D-decylmaltoside, pH 8.0, and reconcentrated as before. If necessary, further concentration was performed with Nanosep tubes (Pall) for 10–20 min at room temperature on a benchtop centrifuge at 13 000 rpm. The purified oxidase was stored at –20 °C.

Gel Electrophoresis and Immunodetection. If not noted otherwise, protein concentration was determined with the bicinchoninic acid (Sigma) method (38) using bovine serum albumin as standard or by visible spectroscopy (see below). SDS–polyacrylamide gel electrophoresis was done as described by Laemmli (39). For immunoblotting, the semidry method was used (Fast Blot apparatus, Biometra) (40); the immunochemical detection of cytochrome *bo*₃ made with rabbit serum specific for subunit II (kindly donated by Drs. Lappalainen and Saraste) was performed with alkaline phosphatase-coupled secondary antibody using 5-bromo-4-chloro-3-indolyl phosphate and nitro blue tetrazolium chloride as substrates. The presence of histidine tags on expressed proteins was confirmed with a conjugate recognizing the oligohistidine epitope, Ni²⁺-NTA-HRP (Qiagen), by following the instructions of the manufacturer.

Optical Spectroscopy. Optical redox difference spectroscopy for qualitative and quantitative characterization of oxidase was performed by an Aminco DW-2 spectrophotometer in the split-beam mode. Dithionite-reduced minus air-oxidized spectra were recorded, and the amount of oxidase in membrane-bound and soluble forms was determined by using an extinction coefficient $\Delta\epsilon_{560-580}$ of 18.7 mM^{–1} cm^{–1} (26).

Measurement of Enzyme Activity. The *in vivo* activity assay of cytochrome oxidase, based on complementation of respiratory-deficient host strains, was performed as described in (37). The cytochrome *bo*₃ oxidase activity test was done with the Aminco DW-2 spectrophotometer in the dual wavelength mode. Incubations were made routinely at 20 °C in a buffer containing 50 mM potassium phosphate, pH 7.0, 1 mM EDTA, 0.3% β -D-decylmaltoside, and 200 μ g/mL α -phosphatidylcholine (Sigma), using the artificial substrate duroquinol at 200 μ M, generated by reducing duroquinone (2,3,5,6-tetramethyl-*p*-benzoquinone) with molecular hydrogen (the product was a kind donation of Prof. Oettmeier). Substrate oxidation was observed by changes in

the absorbance difference in the ultraviolet after addition of duroquinol, using the extinction coefficient $\Delta\epsilon_{270-285}$ of 19.4 mM^{–1} cm^{–1} (41).

Optical and FTIR Spectroscopy and Heme Analysis. Samples for FTIR spectroscopy were prepared as described in (42) without glycerol treatment. Spectra with a nominal resolution of 4 cm^{–1} were recorded at –40 °C and are displayed as difference spectra taken before and after laser flash photolysis at 540 nm; 80 interferograms after light flash were sampled, and the data resulting from 1000 flashes were averaged. Hemes were extracted and analyzed as described in ref 43.

Mass Spectroscopic Methods. ESI mass spectrometry was done as described in ref 44. A sample aliquot of 2 pmol was washed several times on an Amicon filter membrane (cutoff 10 kDa) with acetonitrile/H₂O and 0.5% formic acid to remove salt and detergents. Then the purified sample was transferred to a nanospray capillary. Mass spectroscopic measurements were done on a Micromass Q-TOF Instrument. The data were analyzed using the MaxEnt algorithm (45).

RESULTS

Construction of pHTAG and Expression of Cytochrome *bo*₃. We constructed a cytochrome *bo*₃ oxidase variant tagged with oligohistidines at the C-terminus of subunit IV (CyoD) for better binding to a metal affinity column and for the study of posttranslational modifications in subunit II. Using the overlap extension PCR method, we made the plasmid pHTAG, intended to code for a six histidine extension. Surprisingly, nucleotide sequencing of the reconstructed plasmid region predicted the presence of seven histidines at the C-terminus of subunit IV, in addition to the natural C-terminal histidine. A total of eight histidines suggests that one additional codon was introduced, because oligonucleotide primer annealing within the highly repetitive region (Table 1) led to variable overlap. Otherwise, the DNA sequence verified the desired construct. The vector pHTAG is based on extension of pMC39 (34), the latter being regarded as wild-type plasmid. It contains the structural genes *cyoA* (subunit II), *cyoB* (subunit I), *cyoC* (subunit III), *cyoD* (subunit IV), and *cyoE* (encoding farnesyltransferase necessary for heme O biosynthesis) (Figure 1). The construct is a medium copy vector permitting the expression of oxidase from its authentic promoter. In fact, the promoter region is slightly altered by one base exchange and one base insertion [Lemieux, L. (1992) Ph.D. Thesis, University of Illinois]. These modifications are probably responsible for lowering of promoter strength, which made it possible to clone the plasmid aerobically (46, 47). Cells harboring the vector pHTAG synthesize cytochrome *bo*₃ at elevated levels, which is seen from the red-colored cell pellets after centrifugation. Transformation with pHTAG of a respiration-deficient host strain JM 107 $\Delta\Delta$ and overnight growth on agar LB plates resulted in colonies of a size comparable to the pMC39 control, indicating normal biological function of the respiratory proton pump cytochrome *bo*₃ (Table 2). The cells even grow, if in addition to the C-terminal oligohistidine extension, the *cyoA* and *cyoB* genes were modified in plasmid pHHT to encode a fusion polypeptide of subunits I and II, similar to an earlier report (35). Another construct bearing an oligohistidine tag at the C-terminus of subunit II, pHCL (37,

Table 2: Activity of Cytochrome *bo*₃ Variants

cytochrome <i>bo</i> ₃ expressed from plasmid construct	property ^a	complementation of oxidase double mutant ^b	duroquinol oxidase activity ^c (%)
pHCL	codes for oligohistidine tag at C-terminus of subunit II	+	100
pSTAG	deletion of gene encoding subunit I (<i>cyoB</i>)	—	0
pMC39	wild type (no oligohistidine tag)	+	45
pHTAG	codes for oligohistidine tag at C-terminus of subunit IV	+	48
pFHT	codes for fusion of subunit I + subunit II plus oligohistidine tag at subunit IV	+	23

^a Because of the copy number of the pBR322-based vectors, all constructed strains are overproducers of cytochrome *bo*₃ (except pSTAG).

^b Complementation was tested by transformation of the respective plasmid into the respiratory-deficient host strain *E. coli* JM107ΔΔ and streaked out on LB agarose plates with 100 μg/mL ampicillin, 50 μg/mL kanamycin, and 50 μg/mL chloramphenicol. Plasmids were regarded as complementing (“+”) when colonies appeared visible after overnight incubation at 37 °C. ^c Activity with the enzyme expressed from pHCL was used as a control for duroquinol oxidase; 100% corresponds to 88 ± 2 (*n* = 3) electrons per second.

48), complements like wild-type plasmid. Cells with disrupted *CyoB* did not yield viable cells; therefore, we used plasmid pSTAG, produced by deletion of the *Bg*/II fragment, as a negative control in complementation tests.

Purification and Protein Chemical Characterization. The enzymes expressed from the plasmids pHTAG, pHCL, pMC39, and pFHT were purified. After membrane solubilization with nonionic detergents, cytochrome *bo*₃ from the extracts was selectively bound to an immobilized metal affinity column and eluted with increasing concentrations of imidazol. We used buffer containing 10 and 20 mM imidazol as a washing solvent to displace nonoxidase protein from binding sites on the column. Higher concentrations of imidazol were necessary to elute the oligohistidine-tagged oxidases; we routinely applied a step gradient of 100 mM imidazol to completely wash off the oxidase from the column. To our surprise, we could also purify nontagged variants of cytochrome *bo*₃ with this protocol (see below).

The preparations were characterized with various biochemical and biophysical methods. As expected, heme quantifications verified equal numbers of heme B and O for the protein expressed from pHCL, whereas the pHTAG- and pMC39-derived preparations revealed a significant and reproducible excess of heme O (data not shown). In optical spectra of the purified proteins, depicted in Figure 2a, slight shoulders of the alpha absorbance peaks of the pHTAG- and pMC39-expressed protein can be noted and should be compared to the symmetric band corresponding to the product of pHCL. Cryo-FTIR difference spectra (42) of carbon monoxide bound to the protein demonstrate that the binuclear centers of these different oxidase constructs behave like wild type (Figure 2b), showing the known bands of 1959 cm⁻¹ for the heme-iron carbonyl (dark) and the copper carbonyl at 2063 cm⁻¹ (light).

The quinol oxidase activity of the purified enzymes was tested with the artificial substrate duroquinol (Table 2). Turnover numbers obtained with purified cytochrome *bo*₃ are similar to those found for the membrane-bound enzyme (41). However, the rates are much lower than those reported for the hydrophobic substrates ubiquinol and decylubiquinol (31, 49). Interestingly, the highest turnover was measured with the subunit II-tagged oxidase. The pH optimum for this reaction was at 7.5, and full inhibition after addition of 2 mM cyanide was observed. As expected for a membrane protein, the activities of the soluble oxidase could be increased by a factor of 5 in the presence of at least 50 μg/

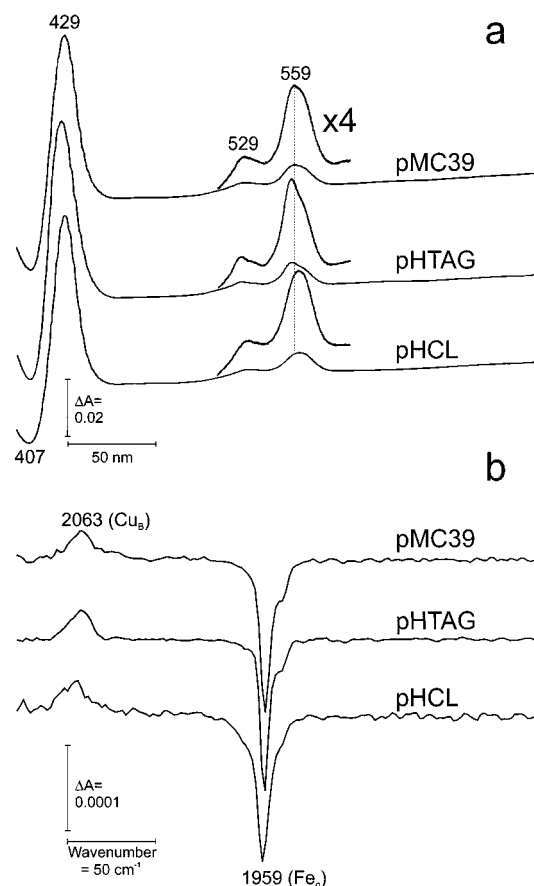


FIGURE 2: Spectroscopical characterization of the pHCL-, pMC39- and pHTAG-derived oxidases. (a) Optical difference spectra of dithionite-reduced minus air-oxidized cytochrome *bo*₃ recorded at room temperature. The cuvettes contained 0.7 μM purified cytochrome *bo*₃. (b) Cryo-FTIR difference spectra of carbon monoxide binding to membrane-bound cytochrome *bo*₃ (light minus dark).

mL phosphatidylcholine. The Michaelis–Menten constants *K_m* with duroquinol for the products expressed from pHCL and pHTAG were on the order of 170–200 μM (data not shown).

Table 3 documents the stepwise purification of oxidase expressed from the plasmid pHTAG, which is further underlined by a typical electrophoresis gel (Figure 3). The apparent polypeptide masses range from 60 (subunit I), 32–33 (subunit II), 22 (subunit III) and 17 kDa (subunit IV, histidine-tagged). In contrast to the sharp double band of subunit II (see below), the blurred bands of subunits I, III,

Table 3: Purification of Cytochrome *bo*₃ Expressed from BL21Δ*cyo* *recA*[−]/pHTAG

sample	cytochrome <i>b</i> ^a (nmol)	total protein (mg)	nmol of cytochrome <i>b</i> / mg of protein	enrichment factor
membranes after urea treatment	155.0 (100%)	139.0	1.1	1.0
detergent extract	112.0 (72%)	61.0	1.8	1.6
Ni ²⁺ -NTA-agarose flow through	50.0 (32%)	34.0	1.5	1.3
Ni ²⁺ -NTA-agarose eluate	34.5 (22%)	4.6	7.5	6.7

^a Cytochrome *b* was quantified spectroscopically by using the extinction coefficient of cytochrome *bo*₃ (see Materials and Methods).

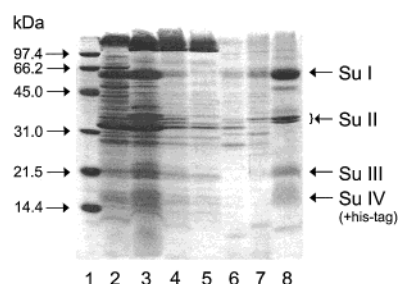


FIGURE 3: SDS-PAGE (15%) showing the progress of purification of cytochrome *bo*₃ tagged with oligohistidine at subunit IV, stained with Coomassie Brilliant Blue R250. Lane 1, molecular mass marker proteins (Bio-Rad); lane 2, membranes before urea treatment; lane 3, membranes after urea treatment; lane 4, supernatant after detergent solubilization; lane 5, flow through after NTA-agarose column loading; lane 6, second wash step (10 mM imidazol); lane 7, third wash step (20 mM imidazol); and lane 8, concentrated cytochrome *bo*₃ oxidase after elution with 100 mM imidazol.

and IV may be due to their high content of hydrophobic amino acids.

Posttranslational Modifications of Subunits II, III, and IV. Electrospray ionization is a mass spectrometrical method that allows the determination of polypeptide masses with the highest precision and in the mass range of larger proteins (50). The protein solution passes an electrostatic field generating positively charged droplets. These droplets shrink by solvent evaporation until an ion release from the liquid surface occurs. The multiply charged ions enter the mass analyzer, where their mass-to-charge ratio and thereby the molecular weight of the protein can be determined. The original mass spectra obtained for cytochrome *bo*₃, expressed from pHTAG, are shown in Figure 4. A number of positively charged ions, denoted A to F, are observed as ensembles of their *n*-fold protonated derivatives. After deconvolution of the data, each ion signal can be assigned to one of the constituent polypeptides of the oxidase (Figure 5b). Ion series are resolved to (A) subunit IV (oligohistidine-tagged), (B) a possible artifact, (C and D) subunit III, and (E and F) subunit II (Table 4). Subunit I could not be identified by ESI mass spectroscopy, probably because the ionization was suppressed by its enormous hydrophobicity. Clearly, the designed attachment of seven histidine residues (959 Da) to the C-terminus of subunit IV is verified. Moreover, it can be seen that the N-terminal methionine residue is split off posttranslationally.

The occurrence of two peaks relating to subunit III (Figure 5a) is highly unexpected, both resulting from polypeptides, in which the N-terminal methionine is split off. The masses corresponding to the observed peaks differ by 41 Da, which is exactly the mass of an acetyl group. The integral band intensity is the same for both signals. This suggests that 50%

of the subunit III polypeptides of cytochrome *bo*₃ is acetylated.

The presence of more than one band corresponding to subunit II is less surprising, because this is already obvious from the gel electrophoretic pattern (Figure 3). However, none of the observed peaks match the theoretical mass derived from sequencing (Table 4). The masses of 33 009 and 32 378 Da of the proteins F and E are lower than the theoretical value, indicating that both represent posttranslationally modified forms. Subunit II has the recognition site of a lipoprotein at amino acid positions 22–25 (51), the so-called “lipo-box” with the amino acid sequence LSGC. If only the predicted signal peptide (amino acids 1–24) with a mass of 2694 Da is split off, a residual mass of 32 217 Da would result. Thus, according to the proposed lipoprotein processing mechanism (52), it has to be postulated that low molecular mass compounds (glycerol plus fatty acids) are linked to the fragment released from its signal peptide. In fact, an extra mass predicted to be a direct consequence of lipid attachment of 792 Da is determined for the heavier fragment with the ESI technique. A number of microbial lipoproteins are modified by an acyl plus a diacylglyceryl group at the N-terminal cysteines (53). For 65% of modifications, the N-linked group is palmitic acid in the *E. coli* murein-lipoprotein (54), which can be considered as a prototype. Moreover, similar to the phospholipid composition of *E. coli*, the main fatty acid of the diacylglyceryl group is palmitic acid (53%) as well (54), and it has been shown that subunit II can incorporate radioactively labeled palmitic acid (51). Assuming that palmitate also provides the natural modification, a mass increase of palmitoyl (mass: 239 Da) plus dipalmitoylglyceryl (mass: 552 Da) groups would be expected, the sum of which amounts to an expected mass of 791 Da, which closely matches to the measured difference of 792 Da. We conclude that, most probably, the 33 009-Da polypeptide represents the processed lipoprotein, which after cleavage of the signal peptide carries an N-palmitoyl and a S-dipalmitoylglyceryl modification at its cysteine at position number 1.

The same calculation for the smaller polypeptide variant of subunit II (32 378 Da) leads to an extra mass of 161 Da, which cannot readily be assigned to a lipid modification. The development of this polypeptide is highly dependent on the growth phase of the bacteria (31), as can be seen from the immunoblot in Figure 6. Significant formation starts about 8 h after inoculation and continues steadily to the stationary phase. Since additional smaller fragments occur at later stages, the effect is explained as a proteolytic event. To exclude that proteolysis takes place at the N-terminus of the protein, we compared the cytochrome *bo*₃ oxidases modified with oligohistidine at the C-terminus of subunit II (expressed from plasmid pHCL) and subunit IV (expressed

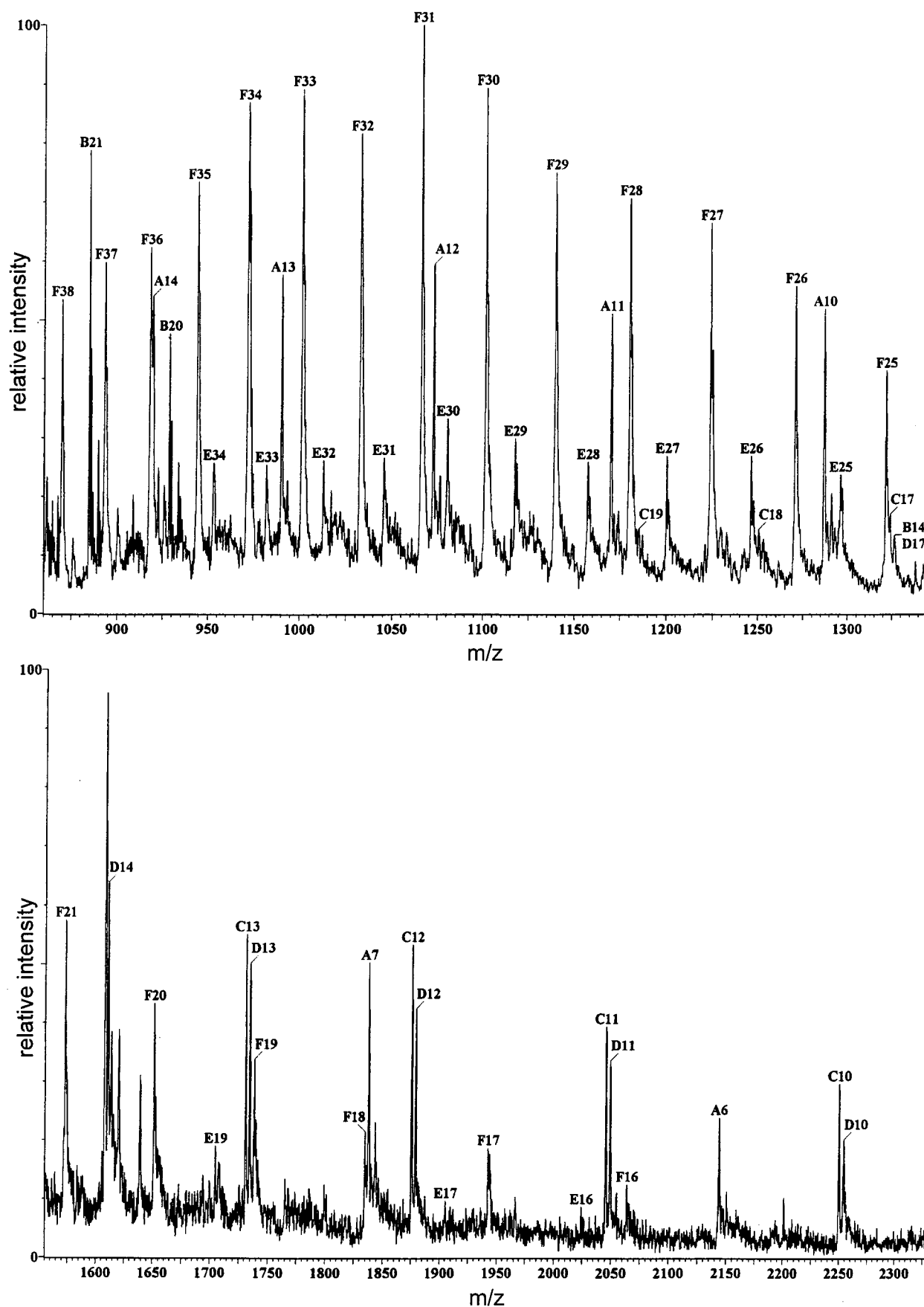


FIGURE 4: ESI mass spectra of purified cytochrome *bo*₃. Original mass spectra magnified in two significant parts of the observed *m/z* range. The multiply charged ion series are attached to the cytochrome *bo*₃ subunits as follows: A, subunit IV with oligohistidine tag; B, an artifact with only two ion signals; C, subunit III without N-terminal methionine; D, acetylated subunit III without N-terminal methionine; E, subunit II without C-terminal hexapeptide; F, subunit II uncleaved.

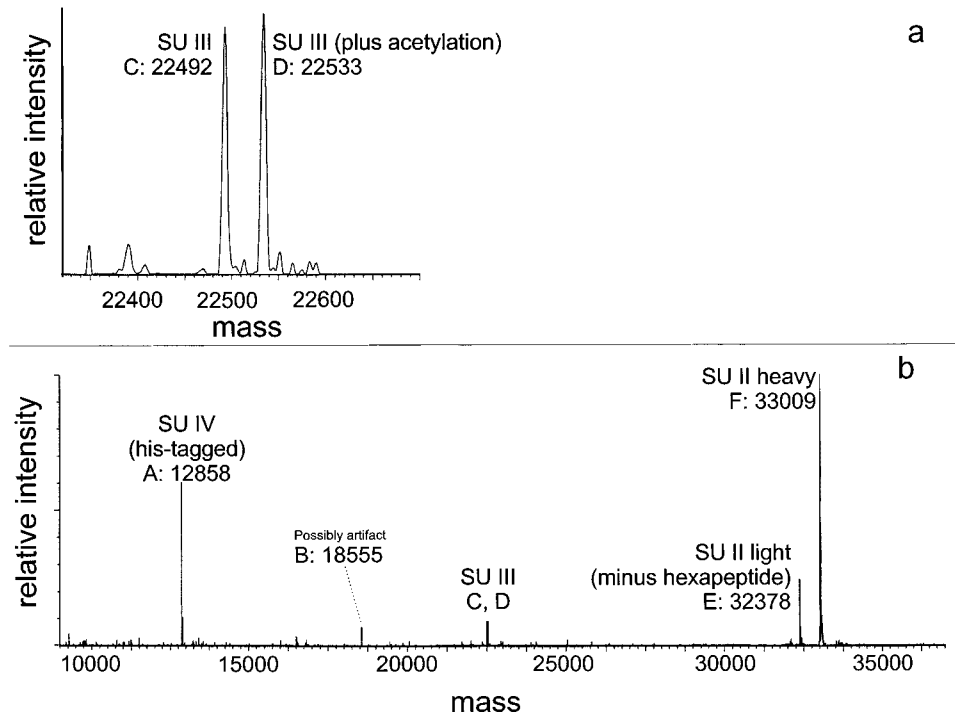


FIGURE 5: ESI mass spectrum of purified cytochrome *bo*₃, shown after deconvolution of the data from Figure 4 with the MaxEnt algorithm (45).

Table 4: Mass Determination by ESI Mass Spectroscopy

subunit	molar mass (calcd from sequence) (Da)	subunit masses ^a assigned from ESI-MS (Da)	comments
I (CyoB)	74 367	nd	
II (CyoA)	34 911	F: 33 009 (75%) ^{b,c} E: 32 378 (25%) ^{b,c}	F: uncleaved E: hexapeptide cleaved from C-terminus
III (CyoC)	22 491 (–Met)	C: 22 492 (50%) ^b D: 22 533 (50%) ^b	D: plus 41 Da acetyl group
IV (CyoD)	11 898 (–Met)	nd	
IV (CyoD) + oligohistidine tag	12 857 (–Met) ^d	A: 12 858	addition of 7 histidine residues at the C-terminus

^a The letters correspond to the masses identified in the deconvoluted spectra. ^b The percentage value represents the integrated peak areas. ^c As seen from polyacrylamide gels, the distribution of both variants is variable, depending on the growth state of cells before harvesting. ^d Histidine (*m* = 137 Da, without H₂O); 7 His = 959 Da.

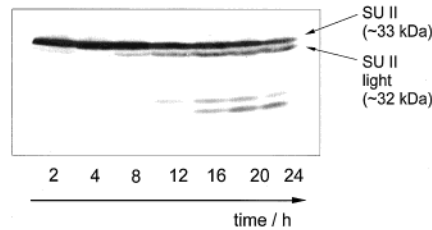


FIGURE 6: Time course of subunit II expression. At indicated times after inoculation, an aliquot of *E. coli* cells expressing the subunit IV-tagged oxidase (equivalent to 12 μ g of protein) was centrifuged and mixed with sample loading buffer for SDS–PAGE. After electrophoresis and electrotransfer, the blot was immunostained with polyclonal antiserum against subunit II.

from plasmid pHTAG) (Figure 7). The histidine-tagged subunit is significantly heavier than the nonmodified protein, as seen in Figure 7A. The cleavage products of tagged and nontagged subunits II run identically. This suggests the formation of identical end products cleaved at the C-terminus of subunit II. The oligohistidine tag is absent in the smaller polypeptide (Figure 7C), clearly demonstrating that the proteolytic cleavage takes place at the C-terminus of the

protein. The oligohistidine tag of subunit IV of the oxidase expressed from pHTAG cannot be visualized; it probably exhibits poor electroblotting efficiency due to its extreme hydrophobicity and low molecular mass.

The mass difference between both variants of subunit II is (33009 – 32378 Da) 631 Da. Supposing the smaller fragment carries the same lipid attachment to the N-terminus, this mass difference corresponds exactly to the C-terminal hexapeptide, HAESAH. We therefore conclude that the proteolytic cleavage of subunit II happens at a later stage than the posttranslational lipid modification.

DISCUSSION

Immobilized metal affinity columns are useful for the purification of native cytochrome oxidases (29). Binding to the column material is mediated by metal binding sites exposed to the protein surface, but it could be further enhanced after the design of additional binding sites [i.e., by the introduction of a C-terminal extension by oligohistidine (see above)]. After detergent solubilization, cytochrome *bo*₃, tagged at subunits II and IV, could be purified efficiently

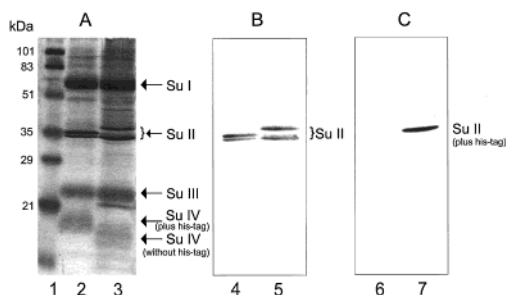


FIGURE 7: C-terminal proteolysis of subunit II. Purified cytochrome *bo*₃, bearing oligohistidine tags at the C-terminus of subunit II and IV (expressed from plasmids pHCL and pHTAG, see text), was separated on an SDS-PAGE gel and electrotransferred on a nitrocellulose membrane. One portion of the gel was stained with Coomassie Brilliant Blue R250 (A: lane 1, molecular weight markers; lane 2, subunit IV-tagged; and lane 3, subunit II-tagged cytochrome *bo*₃; 8 μ g was loaded per lane.) The blot was immunostained with polyclonal antiserum against subunit II (B: lane 4, subunit IV-tagged; and lane 5, subunit II-tagged cytochrome *bo*₃; 1.5 μ g was loaded per lane) and labeled by means of Ni-NTA HRP-conjugate (Qiagen) (C: lane 6, 4 μ g of subunit IV-tagged cytochrome *bo*₃; and lane 7, 2 μ g of subunit II-tagged cytochrome *bo*₃).

in a one-step process. Possible proteolysis has been suggested to explain the heterogeneity of subunit II (31); our present study demonstrates the applicability of the procedure irrespective of posttranslational changes. Functional oxidase could be prepared even when growth conditions described above led to partial loss of the histidine tag of subunit II, because in the presence of 20 mM imidazol the nontagged material remains bound to the column. Using the same approach, we were even able to purify the wild-type cytochrome oxidase encoded by the plasmid pMC39. In contrast to other authors (31, 51) who purified exclusively the unprocessed forms, we explain our results by assuming that the oxidase solubilized from urea-treated membranes binds to the column if imidazol is omitted from the equilibration buffer. This notion is supported by another finding that nontagged cytochrome *bo*₃ binds to metal affinity matrixes (29).

Initially, we favored to work with cytochrome *bo*₃, which is histidine tagged at subunit IV, because we wished (i) to carry out structural studies with the protein containing fused subunits I and II (as for example, expressed from pFHT) and (ii) to provide an efficient purification system for a number of site-directed mutants. The activity of the protein expressed from pHTAG has 50% activity of the subunit II-tagged oxidase. The subunit IV-tagged fusion protein, connecting the C-terminus of subunit II with the N-terminus of subunit I exhibits only 20% of control activity. Surprisingly, the nontagged "wild-type" oxidase expressed from pMC39 exhibited about 50% of the pHCL-derived activity (Table 2). It should be noted that these enzymes were purified after Triton X-100 solubilization of cytoplasmic membranes, which is responsible for the removal of the tightly bound ubiquinol molecule, which may be responsible for altered enzyme kinetic behavior (48). Initially, we ascribed the low duroquinol oxidase activity to deficient incorporation or destabilization of cofactors, namely of Cu_B, as reasoned before (20). However, the optical CO binding spectra of the reduced samples (pMC39, pHTAG, and pHCL) show the presence of high-spin heme bound at the same stoichiometry to the proteins. Most importantly, carbon monoxide binding

observed by Fourier transform infrared spectroscopy (42) at cryogenic temperatures revealed that high-spin heme and Cu_B are properly inserted in wild-type proportions. Quantitative analysis of heme composition of the purified oxidases by HPLC analysis (31, 43, 55) demonstrated that pHCL oxidase has a 1:1 composition of heme B/heme O, whereas the pMC39 and the pHTAG enzymes have heme O also bound to 50% of the low-spin sites, which are normally exclusively occupied with the heme B species. Heme promiscuity has been related earlier to host-strain properties (55) but was also recently found with cytochrome *bo*₃ tagged at the C-terminus of subunit I (31). It is known that the biophysical properties such as electron-transfer rates are affected by the heme composition (see ref 56 and references therein). To explain our lowered enzyme activities (with the artificial substrate duroquinol) of the pMC39- and pHTAG-derived proteins, we assume that the detergent-induced loss of the tightly bound ubiquinol combined with heme O binding at the low-spin site could be inhibitory. Even though the wild-type based constructs (pMC39, pHTAG) may also have diminished turnover rates in vivo, the aerobic complementation data establish that sufficient oxidase activity is retained to support proton pumping. On the other hand, our site-directed mutations designed into the pHTAG construct at essential positions of subunit I (e.g., Lys-362, Glu-286) resulted in very low expression (unpublished data). If proteins intended to be expressed were mutagenized at critical sites, deleterious effects were probably enhanced. These problems did not occur with mutagenized cytochrome *bo*₃ tagged at the C-terminus of subunit II (37).

ESI mass spectroscopy provides very precise mass values that allow a more correct molecular characterization. Several posttranslational modifications of different subunits could be detected, such as the removal of the N-terminal methionine of subunits III and IV due to methionine aminopeptidase (57). The detection of only 50% acetylation of subunit III molecules is an unexpected result. Probably the acetyl group is bound to the N-terminal alanine, which is preferably labeled, if the amino group becomes accessible after the exoproteolytic elimination of methionine (58, 59). The exact role of this modification is unknown; it may be a signal for degradation of the protein (60). Interestingly, acetylations have been observed in another protein from *E. coli*, SecB (61). More than half of the SecB monomers of the oligomeric complex were acetylated. It is thus tempting to speculate that subunit III of cytochrome *bo*₃ of *E. coli* is dimeric in the isolated oxidase complex, with only one of these monomers being acetylated. However, no hint of dimerization is given by either biochemical data (62) or from the 6-Å electron microscopic projection structure (63). It is also possible that the modifying enzyme N^α-acetyl transferase (57) has restricted access to subunit III during biosynthesis and assembly of the oxidase.

Basic lipoprotein features could be ascribed to subunit II from molecular sequence and biochemical data. However, no X-ray structure is published for cytochrome *bo*₃. As yet, no specific information on the lipid structure has been obtained. Lipid structures of lipoproteins have been determined by chemical methods or were derived from data on phospholipid composition. Our data on the structure of the lipid modification are fully consistent with palmitic acid being the main constituent. However, some minor variations

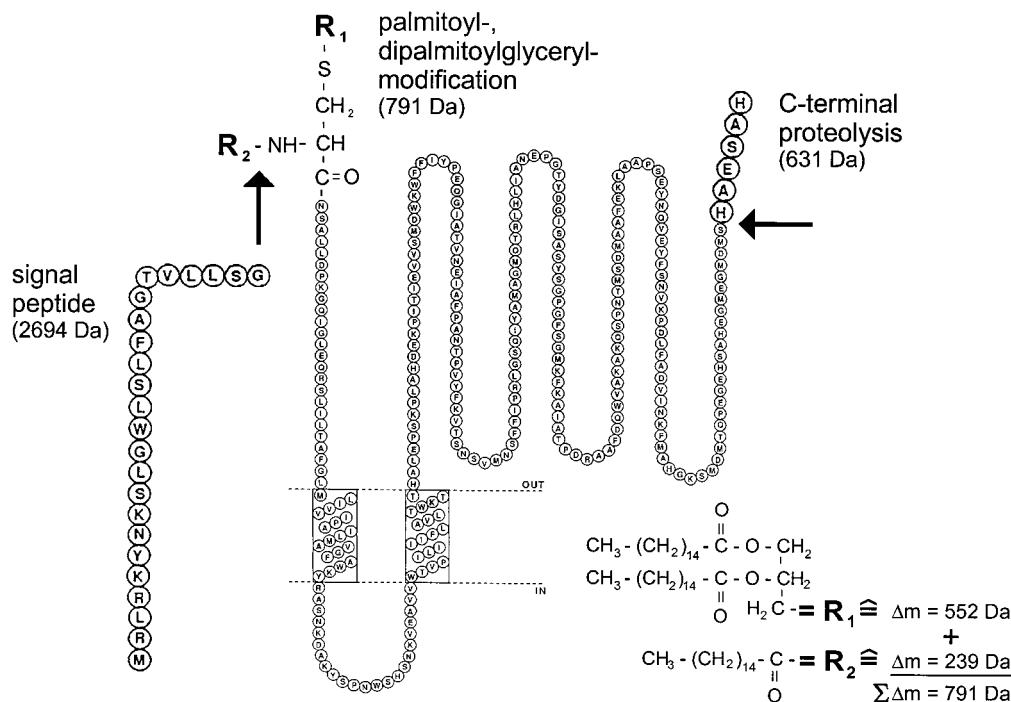


FIGURE 8: Summary of posttranslational modifications of subunit II (CyoA) of cytochrome bo_3 of *E. coli*. This model is based on the CyoA topology data determined in ref 8.

in the fatty acid distribution might be recognized from the very small broadening of the ESI peak width of the subunit II-related mass peaks E and F in Figure 4. This could indicate that a tiny fraction of the bound lipid exhibits limited structural heterogeneity.

Regarding the principal lipid component, we could demonstrate for the first time with high-precision mass spectroscopy that the N-terminal cysteine of CyoA carries an N-palmitoyl and an S-dipalmitoylglyceryl modification. The sequence of lipoprotein processing events, analogous to outer membrane proteins (52), were adapted to subunit II and summarized in Figure 8. After attachment of the dipalmitoylglyceryl group to the SH group of Cys-25, the signal peptide is cleaved off, and then the newly created N-terminal amino group is palmitoylated. A third event is the cleavage of the C-terminal hexapeptide, HAESA_H, which takes place after the N-terminal processing steps.

The reason for C-terminal peptide cleavage is unknown. Splitting of a much longer peptide has been observed for subunit II of *Paracoccus* cytochrome *c* oxidase (64). The C-terminal proteolysis of CyoA happens in vivo. Proteolysis is not necessary for activity of the protein, because the fusion protein connecting subunits I and II (pFHT construct) is enzymatically active. The hexapeptide of the fusion protein is probably buried in the fusion protein: it is not cleaved in vivo, which indicates that the peptide must be exposed to allow access of a cleaving protease. The hexapeptide is not necessary for enzyme activity, because the purified cytochrome *bo*₃ with the cleaved hexapeptide did not show significant loss of activity (A.P. and M.L., unpublished data).

The function of the lipoprotein modification is unknown. Since CyoA has two transmembrane segments (8), it would not be necessary to stabilize membrane binding by introduction of an extra membrane anchor. The modified lipid could be involved in protein-protein recognition (65). An earlier report suggests that the oxidase is still functional after

mutation of signal peptide at critical sites (51). The lipoprotein features of subunit II may thus be related to a regulatory phenomenon in the bacteria.

ACKNOWLEDGMENT

We thank Dr. Dietrich Kuschmitz (Max-Planck-Institut für Molekulare Physiologie, Dortmund) for support with fermentation.

REFERENCES

1. Saraste, M. (1990) *Q. Rev. Biophys.* 23, 331–66.
2. Saraste, M., Holm, L., Lemieux, L., Lübben, M., and van der Oost, J. (1991) *Biochem. Soc. Trans.* 19, 608–12.
3. Lübben, M. (1995) *Biochim. Biophys. Acta* 1229, 1–22.
4. Garcia-Horsman, J. A., Barquera, B., Rumbley, J., Ma, J., and Gennis, R. B. (1994) *J. Bacteriol.* 176, 5587–600.
5. Ferguson-Miller, S., and Babcock, G. T. (1996) *Chem. Rev.* 96, 2889–907.
6. Iwata, S., Ostermeier, C., Ludwig, B., and Michel, H. (1995) *Nature* 376, 660–9.
7. Tsukihara, T., Aoyama, H., Yamashita, E., Tomizaki, T., Yamaguchi, H., Shinzawa-Itoh, K., Nakashima, R., Yaono, R., and Yoshikawa, S. (1996) *Science* 272, 1136–44.
8. Chepuri, V., and Gennis, R. B. (1990) *J. Biol. Chem.* 265, 12978–86.
9. Lappalainen, P., Watmough, N. J., Greenwood, C., and Saraste, M. (1995) *Biochemistry* 34, 5824–30.
10. Witt, H., Malatesta, F., Nicoletti, F., Brunori, M., and Ludwig, B. (1998) *Eur. J. Biochem.* 251, 367–73.
11. Kelly, M., Lappalainen, P., Talbo, G., Haltia, T., van der Oost, J., and Saraste, M. (1993) *J. Biol. Chem.* 268, 16781–7.
12. van der Oost, J., Lappalainen, P., Musacchio, A., Warne, A., Lemieux, L., Rumbley, J., Gennis, R. B., Aasa, R., Pascher, T., Malmström, B. G., and et al. (1992) *EMBO J.* 11, 3209–17.
13. Richter, O. M., Tao, J. S., Turba, A., and Ludwig, B. (1994) *J. Biol. Chem.* 269, 23079–86.
14. Lübben, M., Warne, A., Albracht, S. P., and Saraste, M. (1994) *Mol. Microbiol.* 13, 327–35.

15. Surpin, M. A., Lübben, M., and Maier, R. J. (1996) *Gene* 183, 201–6.
16. Tsatsos, P. H., Reynolds, K., Nickels, E. F., He, D. Y., Yu, C. A., and Gennis, R. B. (1998) *Biochemistry* 37, 9884–8.
17. Nalecz, K. A., Bolli, R., Ludwig, B., and Azzi, A. (1985) *Biochim. Biophys. Acta* 808, 259–72.
18. Haltia, T., Finel, M., Harms, N., Nakari, T., Raitio, M., Wikström, M., and Saraste, M. (1989) *EMBO J.* 8, 3571–9.
19. Villani, G., Tattoli, M., Capitanio, N., Glaser, P., Papa, S., and Danchin, A. (1995) *Biochim. Biophys. Acta* 1232, 67–74.
20. Saiki, K., Nakamura, H., Mogi, T., and Anraku, Y. (1996) *J. Biol. Chem.* 271, 15336–40.
21. Nakamura, H., Saiki, K., Mogi, T., and Anraku, Y. (1997) *J. Biochem. (Tokyo)* 122, 415–21.
22. Chepuri, V., Lemieux, L., Au, D. C., and Gennis, R. B. (1990) *J. Biol. Chem.* 265, 11185–92.
23. Minghetti, K. C., Goswitz, V. C., Gabriel, N. E., Hill, J. J., Barassi, C. A., Georgiou, C. D., Chan, S. I., and Gennis, R. B. (1992) *Biochemistry* 31, 6917–24.
24. Ludwig, B., and Schatz, G. (1980) *Proc. Natl. Acad. Sci. U.S.A.* 77, 196–200.
25. Gennis, R. B., Casey, R. P., Azzi, A., and Ludwig, B. (1982) *Eur. J. Biochem.* 125, 189–95.
26. Kita, K., Konishi, K., and Anraku, Y. (1984) *J. Biol. Chem.* 259, 3368–74.
27. Azzi, A., and Gennis, R. B. (1986) *Methods Enzymol.* 126, 138–45.
28. Lübben, M., Arnaud, S., Castresana, J., Warne, A., Albracht, S. P., and Saraste, M. (1994) *Eur. J. Biochem.* 224, 151–9.
29. Warne, A., Wang, D. N., and Saraste, M. (1995) *Eur. J. Biochem.* 234, 443–51.
30. Mitchell, D. M., and Gennis, R. B. (1995) *FEBS Lett.* 368, 148–50.
31. Rumbley, J. N., Furlong Nickels, E., and Gennis, R. B. (1997) *Biochim. Biophys. Acta* 1340, 131–42.
32. Saiki, K., Mogi, T., Tsubaki, M., Hori, H., and Anraku, Y. (1997) *J. Biol. Chem.* 272, 14721–6.
33. Zhen, Y., Qian, J., Follmann, K., Hayward, T., Nilsson, T., Dahn, M., Hilmi, Y., Hamer, A. G., Hosler, J. P., and Ferguson-Miller, S. (1998) *Protein Expression Purif.* 13, 326–36.
34. Lemieux, L. J., Calhoun, M. W., Thomas, J. W., Ingledew, W. J., and Gennis, R. B. (1992) *J. Biol. Chem.* 267, 2105–13.
35. Ma, J., Lemieux, L., and Gennis, R. B. (1993) *Biochemistry* 32, 7692–7.
36. Horton, R. M., Cai, Z. L., Ho, S. N., and Pease, L. R. (1990) *Biotechniques* 8, 528–35.
37. Lübben, M., Prutsch, A., Mamat, B., and Gerwert, K. (1999) *Biochemistry* 38, 2048–56.
38. Smith, P. K., Krohn, R. I., Hermanson, G. T., Mallia, A. K., Gartner, F. H., Provenzano, M. D., Fujimoto, E. K., Goeke, N. M., Olson, B. J., and Klenk, D. C. (1985) *Anal. Biochem.* 150, 76–85.
39. Laemmli, U. K. (1970) *Nature* 227, 680–5.
40. Kyhse-Andersen, J. (1984) *J. Biochem. Biophys. Methods* 10, 203–9.
41. Moody, A. J., Mitchell, R., Jeal, A. E., and Rich, P. R. (1997) *Biochemical J.* 324, 743–52.
42. Hill, J., Goswitz, V. C., Calhoun, M., Garcia-Horsman, J. A., Lemieux, L., Alben, J. O., and Gennis, R. B. (1992) *Biochemistry* 31, 11435–40.
43. Lübben, M., and Morand, K. (1994) *J. Biol. Chem.* 269, 21473–9.
44. Immmler, D., Gremm, D., Kirsch, D., Spengler, B., Presek, P., and Meyer, H. E. (1998) *Electrophoresis* 19, 1015–23.
45. Almudaris, A., Ashton, D. S., Beddell, C. R., Cooper, D. J., Craig, S. J., and Oliver, R. W. A. (1996) *Eur. Mass Spectrom.* 2, 57–67.
46. Nakamura, H., Yamato, I., Anraku, Y., Lemieux, L., and Gennis, R. B. (1990) *J. Biol. Chem.* 265, 11193–7.
47. Chepuri, V., Lemieux, L., Au, D. C., and Gennis, R. B. (1990) *J. Biol. Chem.* 265, 11185–92.
48. Puustinen, A., Verkhovsky, M. I., Morgan, J. E., Belevich, N. P., and Wikström, M. (1996) *Proc. Natl. Acad. Sci. U.S.A.* 93, 1545–8.
49. Puustinen, A., and Wikström, M. (1999) *Proc. Natl. Acad. Sci. U.S.A.* 96, 35–7.
50. Siethoff, C., Lohaus, C., and Meyer, H. E. (1999) in *Micro-characterization of Proteins* (Kellner, R., Lottspeich, F., and Meyer, H. E., Eds.) pp 245–273, Wiley-VCH Verlag, Weinheim.
51. Ma, J., Katsonouri, A., and Gennis, R. B. (1997) *Biochemistry* 36, 11298–303.
52. Sankaran, K., and Wu, H. C. (1994) *J. Biol. Chem.* 269, 19701–6.
53. Braun, V., and Wu, H. C. (1993) in *Comprehensive Biochemistry* (Ghuysen, J.-M., and Hackenbeckeds, R., Eds.) pp 319–342, Elsevier Science Publishers B. V., Amsterdam.
54. Hantke, K., and Braun, V. (1973) *Eur. J. Biochem.* 34, 284–296.
55. Puustinen, A., Morgan, J. E., Verkhovsky, M., Thomas, J. W., Gennis, R. B., and Wikström, M. (1992) *Biochemistry* 31, 10363–9.
56. Verkhovsky, M. I., Morgan, J. E., Puustinen, A., and Wikström, M. (1996) *Nature* 380, 268–70.
57. Bradshaw, R. A., Brickey, W. W., and Walker, K. W. (1998) *Trends Biochem. Sci.* 23, 263–7.
58. Flinta, C., Persson, B., Jornvall, H., and von Heijne, G. (1986) *Eur. J. Biochem.* 154, 193–6.
59. Persson, B., Flinta, C., von Heijne, G., and Jornvall, H. (1985) *Eur. J. Biochem.* 152, 523–7.
60. Arfin, S. M., Kendall, R. L., Hall, L., Weaver, L. H., Stewart, A. E., Matthews, B. W., and Bradshaw, R. A. (1995) *Proc. Natl. Acad. Sci. U.S.A.* 92, 7714–8.
61. Smith, V. F., Schwartz, B. L., Randall, L. L., and Smith, R. D. (1996) *Protein Sci.* 5, 488–94.
62. Musatov, A., Ortega-Lopez, J., Demeler, B., Osborne, J. P., Gennis, R. B., and Robinson, N. C. (1999) *FEBS Lett.* 457, 153–6.
63. Gohlke, U., Warne, A., and Saraste, M. (1997) *EMBO J.* 16, 1181–8.
64. Steinrück, P., Steffens, G. C., Panskus, G., Buse, G., and Ludwig, B. (1987) *Eur. J. Biochem.* 167, 431–9.
65. Turner, A. J. (1992) in *Lipid Modification of Proteins: A Practical Approach* (Hooper, N. M., Ed.) pp 1–13, IRL Press, Oxford.

BI992193C